Stem Cell Reports
Article

ISSCR

OPEN ACCESS

Competency of iPSC-derived retinas in MHC-mismatched transplantation in non-human primates

Hirofumi Uyama,[1,2,3] Hung-Ya Tu,[1,4] Sunao Sugita,[1,2,5] Suguru Yamasaki,[1,6] Yasuo Kurimoto,[1,2] Take Matsuyama,[1,2] Takashi Shiina,[7] Takehito Watanabe,[8] Masayo Takahashi,[1,2,5] and Michiko Mandai[1,2,*]

[1]Laboratory for Retinal Regeneration, RIKEN Center for Biosystems Dynamics Research, 2-2-3 Minatojima-minamimachi, Chuo-ku, Kobe, Hyogo 650-0047, Japan
[2]Department of Ophthalmology, Kobe City Eye Hospital, 2-1-8 Minatojima-minamimachi, Chuo-ku, Kobe, Hyogo 650-0047, Japan
[3]Graduate School of Medicine, Kyoto University, Kyoto 606-8501, Japan
[4]Laboratory for Molecular and Developmental Biology, Institute for Protein Research, Osaka University, 3-2 Yamadaoka, Suita, Osaka 565-0871, Japan
[5]Vision Care, Inc., Kobe Eye Center 5F, 2-1-8 Minatojima-minamimachi, Chuo-ku, Kobe, Hyogo 650-0047, Japan
[6]Regenerative & Cellular Medicine Kobe Center, Sumitomo Pharma Co., Ltd., Kobe 650-0047, Japan
[7]Department of Molecular Life Science, Division of Basic Medical Science and Molecular Medicine, Tokai University School of Medicine, Isehara 259-1193, Japan
[8]Department of Ophthalmology and Visual Sciences, Graduate School of Biomedical Sciences, Nagasaki University, 1-7-1 Sakamoto, Nagasaki, Nagasaki, 852-8501, Japan
*Correspondence: hirofumi_uyama@kcho.jp (H.U.), e_lab.mandai@kcho.jp (M.M.)
https://doi.org/10.1016/j.stemcr.2022.09.014

SUMMARY

Transplantation of embryonic/induced pluripotent stem cell-derived retina (ESC/iPSC-retina) restores host retinal ganglion cell light responses in end-stage retinal degeneration models with host-graft synapse formation. We studied the immunological features of iPSC-retina transplantation using major histocompatibility complex (MHC)-homozygote monkey iPSC-retinas in monkeys with laser-induced retinal degeneration in MHC-matched and -mismatched transplantation. MHC-mismatched transplantation without immune suppression showed no evident clinical signs of rejection and histologically showed graft maturation without lymphocytic infiltration, although immunological tests using peripheral blood monocytes suggested subclinical rejection in three of four MHC-mismatched monkeys. Although extensive photoreceptor rosette formation was observed on histology, evaluation of functional integration using mouse models such as mouse ESC-retina (C57BL/6) transplanted into rd1(C3H/HeJ, MHC-mismatched model) elicited light responses in the host retinal ganglion cells after transplantation but with less responsiveness than that in rd1-2J mice (C57BL/6, MHC-matched model). These results suggest the reasonable use of ESC/iPSC-retina in MHC-mismatched transplantation, albeit with caution.

INTRODUCTION

Stem-cell-based therapy is a promising approach for restoring and reconstructing visual function in patients with retinal degeneration. The development of innovative protocols for retinal organoid induction from mouse embryonic stem cells (ESCs) (Eiraku et al., 2011), followed by those using human ESCs and induced pluripotent stem cells (iPSCs) (Kuwahara et al., 2015; Meyer et al., 2011; Nakano et al., 2012; Tu et al., 2019; Zhong et al., 2014), has accelerated research on the clinical application of stem-cell-based therapies, with further improvement in differentiation protocols (Kuwahara et al., 2019; Reichman et al., 2017).

In the past decade, transplantation of photoreceptor precursors in retinal degeneration models with a residual outer nuclear layer (ONL) revealed that donor cells can restore the function of host retinas through both direct integration and/or supplying the missing proteins in a phenomenon called "material transfer" (Barber et al., 2013; Gasparini et al., 2022; Gonzalez-Cordero et al., 2013; MacLaren et al., 2006; Ortin-Martinez et al., 2017; Pearson et al., 2012, 2016; Santos-Ferreira et al., 2016; Singh et al., 2013, 2016; Waldron et al., 2018; Warre-Cornish et al., 2014). We and other groups have reported the efficacy of transplantation of retinal sheets or purified photoreceptor precursors from stem-cell-derived retinas for end-stage retinal degeneration with no remaining ONL (Assawachananont et al., 2014; Barnea-Cramer et al., 2016; Iraha et al., 2018; Mandai et al., 2017; Ribeiro et al., 2021; Shirai et al., 2016; Singh et al., 2013; Tu et al., 2019). In particular, we 3-dimensionally identified *de novo* host-graft synapses using a reporter mouse line expressing GFP in rod bipolar cells, reporter grafts expressing the synaptic marker CtBP2:tdTomato in rod photoreceptors, and immunostaining of postsynaptic marker Cacna1s. We also showed that host retinal ganglion cells (RGCs) at the grafted area respond to light using multi-electrode arrays (MEAs) and that transplanted animals better respond to light in behavioral tests (Mandai et al., 2017; Matsuyama et al., 2021). The grafted photoreceptor cells mostly form rosettes but are consistently photoresponsive, even without the addition of 9-*cis* retinal supplementation (Yamasaki et al., 2022). Based on this proof of concept, a clinical trial using human iPSC-retinas for transplantation in patients with retinitis pigmentosa was recently conducted in Japan (jRCTa050200027).

The management of immunological rejection is another critical issue in cell-based therapies. The major histocompatibility complex (MHC) or the human leukocyte

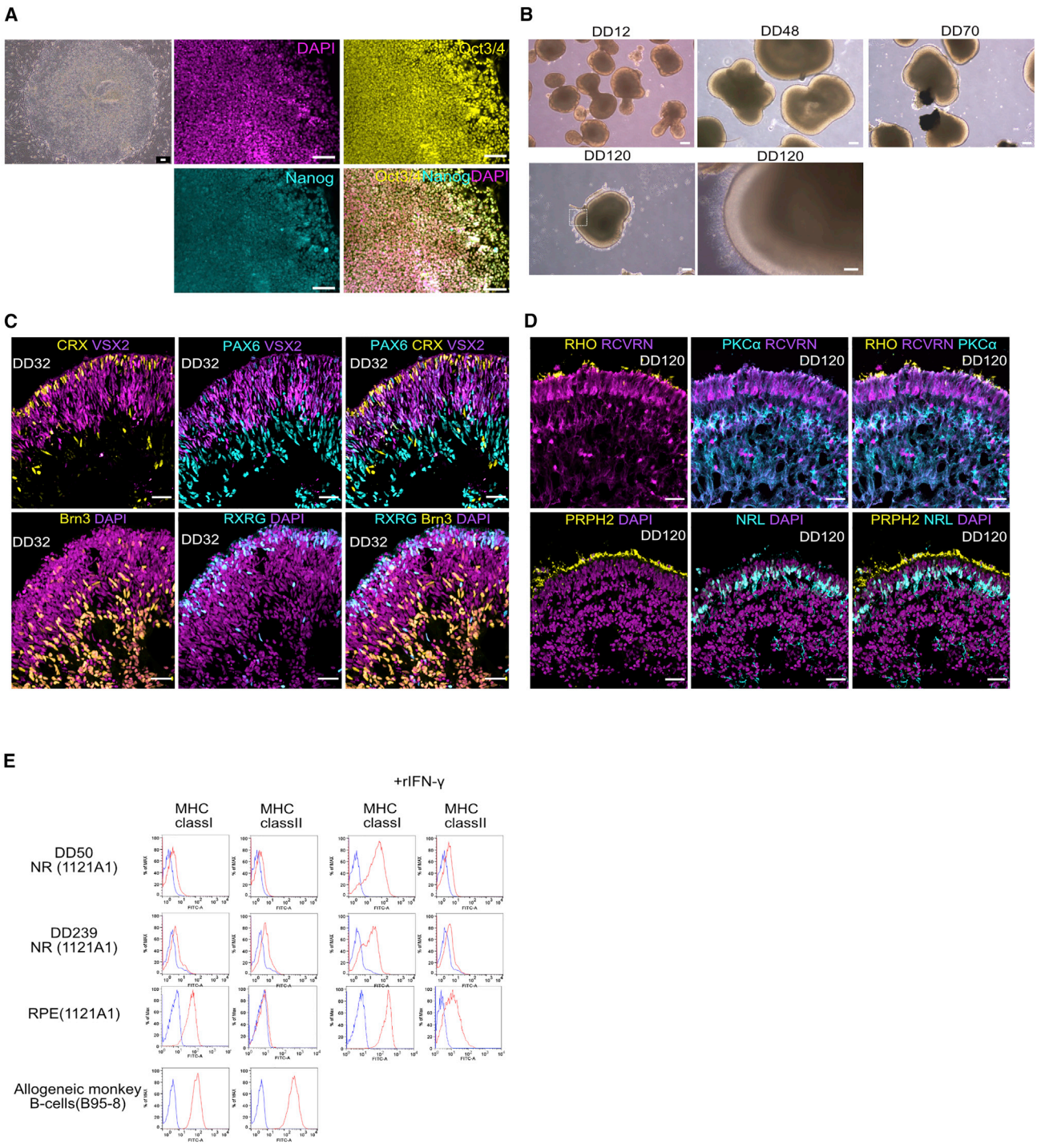

Figure 1. Characterization of monkey 1121A1 MHC homozygous HT1 iPSC retinas

(A) Bright-field image and immunostaining images of the pluripotent stem cell markers in 1121A1-HT1 mkiPSCs.

(B) Bright-field images of DD12–DD120 mkiPSC-retinas during differentiation. Magnified view of a DD120 mkiPSC-retina (white dotted box) presenting fluffy inner segment-like structures.

(C) Immunostaining of DD32 mkiPSC-retinas. (Top panels) PAX6-positive cells are located basal to VSX2-positive retinal progenitor cells. CRX-positive photoreceptor precursor cells are mostly present on the apical side. (Bottom panels) RXRG-positive cone photoreceptor precursor cells and Brn3-positive retinal ganglion cells are observed on the apical and basal sides, respectively.

(legend continued on next page)

antigen (HLA) is a key genetic element in the immune response after transplantation (Petersdorf, 2013). The immunological tolerability of HLA-matched allogeneic transplantation of iPSC/ESC-derived tissues reduces immune cell infiltration and increases graft survival (Morizane et al., 2017; Shiba et al., 2016; Sugita et al., 2016). A bank project to prepare stocks of donor-derived iPSC lines homologous to HLA loci that are highly frequent among the Japanese population now increases the chances of HLA matching for transplantation (Umekage et al., 2019). However, it is expensive to prepare sufficient cell lines.

The eyes are unique immune-privileged sites (Streilein, 2003) that suppress immune responses and actively induce tolerance to foreign antigens (Keino et al., 2018); additionally, they have low immunogenetic properties (Hori et al., 2003). Recently, Yamasaki et al. reported the immunological properties of human ESC/iPSC-retinas, showing low immunogenicity and active features of immunosuppression, partly by the secretion of transforming growth factor β (TGF-β) (Yamasaki et al., 2021). In fact, the long-term survival of transplanted human fetal retinas/retinal cells without systemic immunosuppression has also been reported in patients with retinitis pigmentosa (Das et al., 1999; Radtke et al., 2002). To further assess the immune tolerability of allogenic iPSC-retina transplantation with or without MHC matching, we optimized a differentiation protocol for the MHC homologous monkey iPSC-line (mkiPSC) and compared the immune responses of the host and the graft development between MHC-matched and -mismatched transplantations using the monkey model of laser-induced photoreceptor degeneration (Shirai et al., 2016). We also studied whether functional integration was achieved with or without MHC matching using mouse ESC (mESC) retinas of C57BL/6 for transplantation into the late-stage retinal degeneration mouse models with C57BL/6J or C3H/Hej genetic backgrounds.

RESULTS

Monkey iPSC-derived retinal organoids show low immunogenicity and the potential to functionally integrate after transplantation in rats

The 1121A1 MHC homozygote HT1 mkiPSC line was differentiated into retinas with a characteristic morphology similar to previously reported hESC/iPSC-retinas, and fluffy cilia-like structures were observed on the apical surface at differentiation day 70 (DD70) and DD120 (Figures 1A and 1B). These organoids expressed the retinal progenitor markers PAX6 and VSX2 and photoreceptor precursor marker CRX on DD32. The cone marker RxRG and RGC marker Brn3 were observed in the apical and basal layers, respectively (Figures 1C and 1D). On DD120, PKCα-positive rod bipolar cells and Nrl-positive rod photoreceptor cells were present, and peripherin2 and rhodopsin were localized in the cilia (Figure 1D). In retinal mkiPSCs, on DD50 and DD239, MHC class I expression was lower than that in mkiPSC-retinal pigment epithelial cells (RPEs) or monkey B cells (positive controls) (Sugita et al., 2016), whereas treatment with interferon γ (IFN-γ) enhanced MHC class I expression in mkiPSC-retinal and RPE cells. MHC class II was expressed only in mkiPSC-RPE cells but not in mkiPSC-retinal cells (Figure 1E).

We then examined the competency of the mkiPSC-retina as a graft by transplanting them to 24-week-old SD-Foxn1 Tg (S334ter) 3LavRrrc nude rats, in which most of the rod photoreceptors were lost in the first several weeks of life (Seiler et al., 2014; Tu et al., 2019). We previously showed that ESC/iPSC-retinas transplanted at younger stages develop thick inner nuclear/plexiform layers (INLs/IPLs) to support the ONL, while more developed grafts tend to lose their integrity after transplantation; however, a thick INL may simultaneously hinder the host-graft contact (Assawachananont et al., 2014; Shirai et al., 2016). We therefore tested mkiPSC-retina transplantation at three developmental stages (DD30, DD41, and DD55). The grafts consistently developed rhodopsin-positive photoreceptors at DD126–DD137. As the DD30 grafts developed thick IPLs/INLs, we decided to use DD41–DD55 grafts for following transplantation studies (Figure S1A). We then tested the functional potency of mkiPSC-retinas by isolating dark-adapted grafted retinas from 59- to 60-week-old rats (DD291–DD299) and recorded light responses from the host RGCs using MEA recording systems (n = 4). In contrast to the rarely detected light response in RGCs of degenerated SD-Foxn1 Tg (S334ter) 3LavRrrc rats aged ≥60 weeks (Tu et al., 2019; Yamasaki et al., 2022), two of four transplanted retinas showed evident RGC responses to light over the grafted area (Figure S1B). These

(D) Immunostaining of DD120 mkiPSC-retinas. A RCVRN-positive photoreceptor layer formed on the apical side, which was positive for Nrl. RHO and PRPH2 were localized in the inner segment-like structures on the apical surface. The rod bipolar cell marker PKCα was expressed in the inner cells.

(E) Expression of MHC class I and II by mkiPSC-retinas of immature (DD50) and more mature (DD239) mkiPSC-retinas. MHC class I expression was low in the mkiPSC-retinas (NR), which increased with rIFN-γ treatment, and there was almost no expression of MHC class II. The MHC expression levels of mkiPSC-RPE and B cells (positive control) are presented for comparison. Blue line; isotype control; red line: HLA class I or class II. Scale bars: (A) 100 μm; (B) 200 μm; bottom right panel, 50 μm; (C and D) 30 μm. mkiPSC, monkey iPSC; mkiPSC-retina, monkey iPSC-derived retina; DD, differentiation day; NR, neural retina; MHC, major histocompatibility complex.

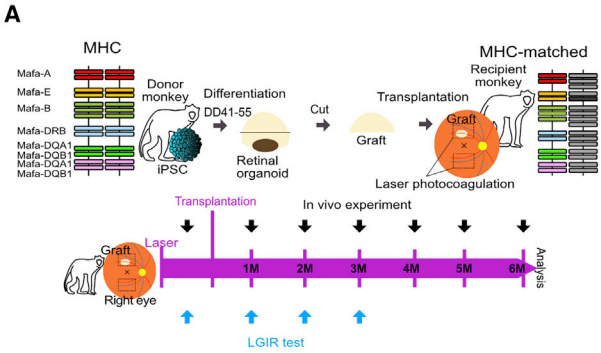

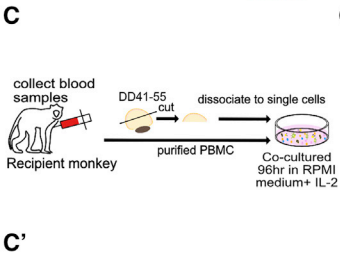

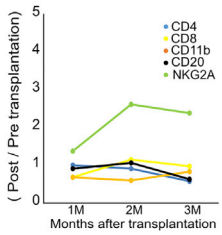

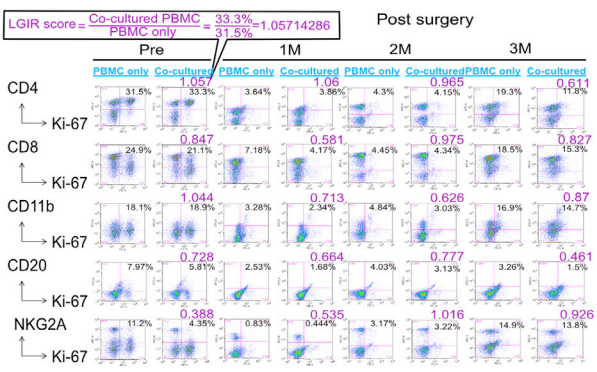

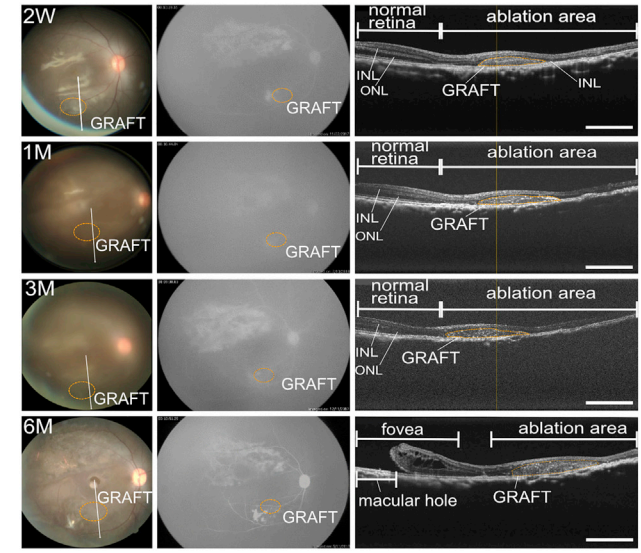

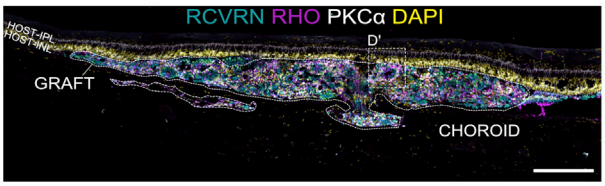

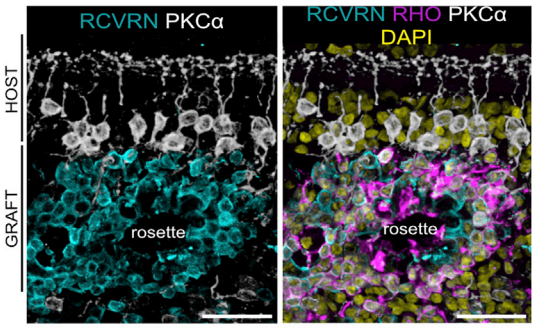

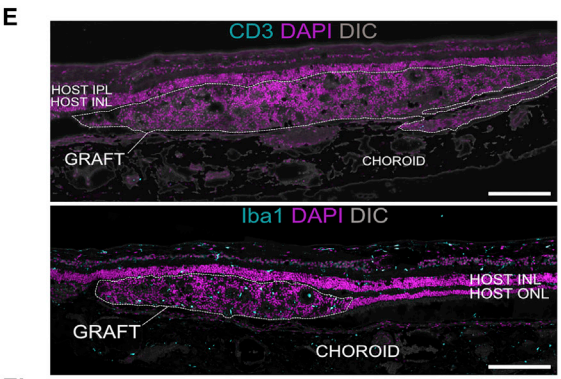

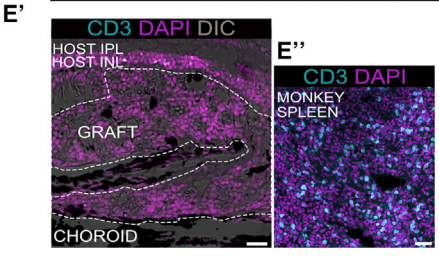

(legend on next page)

indicated that mkiPSC-retinas are useful to study host immune responses to allogenic grafts.

Transplanted MHC-matched grafts survived with no clinical signs of rejection and with negative lymphocyte graft immune reaction tests

We first transplanted mkiPSC-retina into an MHC-matched (10154C) monkey eye after focal laser ONL ablation (Figure 2A). *In vivo* imaging showed stable graft survival with no clinical signs of rejection, such as fluorescein leakage on fluorescein angiography (FAG) or inflammatory responses on optical coherence tomography (OCT) (Figure 2B). Intra-graft speckles on OCT are likely to represent photoreceptor rosettes with inner/outer segment (IS/OS) components and microglia (MG) in later months. We then conducted a lymphocyte graft immune reaction (LGIR) test, which evaluates the proliferation of recipient peripheral blood monocular cells (PBMCs) against mkiPSC-retinas (Sugita et al., 2016) (Figures 2C and S2). Up to 3 months postoperatively, only natural killer cells (NKG2A) exceeded the 2-fold LGIR score, which was judged as negative for rejection (Figures 2C′, 2C″, and S2C). Immunohistochemical staining was positive for mature retinal cell markers, including photoreceptor cells (recoverin and rhodopsin) and rod bipolar cells (PKCα) (Figure 2D). The photoreceptor cell layers developed mostly in a rosette form, showing enhanced rhodopsin expression in the IS/OS-like structures, while some cells expressed rhodopsin on cell membranes. Some photoreceptors in the rosettes were observed to contact the host bipolar cells (Figure 2D′). This was considered important, as we previously observed that contact between the host bipolar cells and graft photoreceptor cells, even in rosette forms, was correlated with host RGC light responses (Yamasaki et al., 2022). Infiltration of CD3-positive T cells in or around the graft were not observed, even in the displaced portion of the choroid. In contrast, ionized calcium-binding adapter molecule 1 (Iba1)-positive MG cells were distributed throughout the graft and inside the graft photoreceptor rosettes (Figures 2E–2E″).

LGIR test revealed subclinical rejection in MHC-mismatched transplantation

Next, we conducted transplantation in four MHC-mismatched monkeys and an additional MHC-matched monkey following the refined study design presented in Figures 3A and 3B. In clinical settings, some patients may wish to receive transplantation in both eyes or do so multiple times; however, a second transplantation may trigger rejection. To test this, the second eye was planned for mkiPSC-retina transplantation 3 months after the first transplantation. A maximum of two retinal grafts were transplanted when the situation allowed for optimization of the multiple sheet transplantation in preparation for clinical application. Table 1 presents the list of monkeys with the observed characteristic features. The haplotypes of the monkeys are summarized in the Table S1. All transplanted eyes (MHC matched or mismatched and without immune suppression) showed no evident clinical signs of rejection, even with repeated transplantation (Figure 3C, and other images in Figures S3 and S4). However, LGIR tests judged that three MHC-mismatched monkeys had subclinical rejection (mismatched

Figure 2. Graft maturation and immune responses in MHC-matched transplantation

(A) Summary of experimental outline for MHC-matched transplantation (top) and *in vivo* examinations and LGIR tests (bottom).

(B) Time course of color fundus photographs and FAG and OCT images after transplantation. Orange circles in fundus images indicate the transplanted graft areas. FAG shows hyper-fluorescence due to RPE atrophy in the laser photocoagulated area. Each OCT image shows the sectional view of the line indicated by the white arrow in the color fundus image. The eye developed a macular hole following the vitrectomy surgery. Grafts survived up to 6 months without evident clinical signs of rejection.

(C–C″) Schematic images of LGIR test (C). Flow cytometry analysis of recipient PBMCs in LGIR test. Fluorescence-activated cell sorting (FACS) plot results of the proliferative population (Ki-67-positive) in each immune cell type as labeled on the left with LGIR score shown above each FACS plot (C′). Ratio changes in LGIR scores of recipients PBMCs at 1, 2, and 3 month posttransplantation (C″). LGIR score increased by more than 2-fold only in NKG2A, and overall LGIR judgment was negative.

(D and D′) Immunostaining of RCVRN (photoreceptors),RHO (rod photoreceptors), and PKCα (rod bipolar cells) after transplantation. Low-magnification image of the transplantation site. Dashed white line indicates the area of the transplant, part of which strays into the choroid (D). Graft photoreceptor cells mostly form rosettes. Magnified view of the photoreceptor rosette adjacent to the host INL (white dotted box in D) (D′). Some photoreceptors express RHO at the outer segment-like structures inside the rosette, whereas others express rhodopsin on the cell membrane. Host PKCα + bipolar cells contact the graft photoreceptor cells.

(E and E′) Immunostaining of CD3 (T cells) and Iba1 (MG). Low-magnification image of the transplantation site (E). The graft is outlined with a dotted white line. There is no evident infiltration of lymphocytes within or around the grafts. MG are observed throughout the graft, mostly inside the rosette. Magnified view of the displaced graft in the choroid in the white dotted box in (E), with no infiltration of lymphocytes (E′). Positive immunostaining for CD3 in a monkey spleen (E″).

Scale bars: (B) 1 mm; (D and E) 200 μm; (D′, E′, and E″) 30 μm. DD, differentiation day; LGIR, lymphocyte graft immune reaction; FAG, fluorescein angiography; OCT, optical coherence tomography; MG, microglia; INL, inner nuclear layer; PBMC, peripheral blood mononuclear cell.

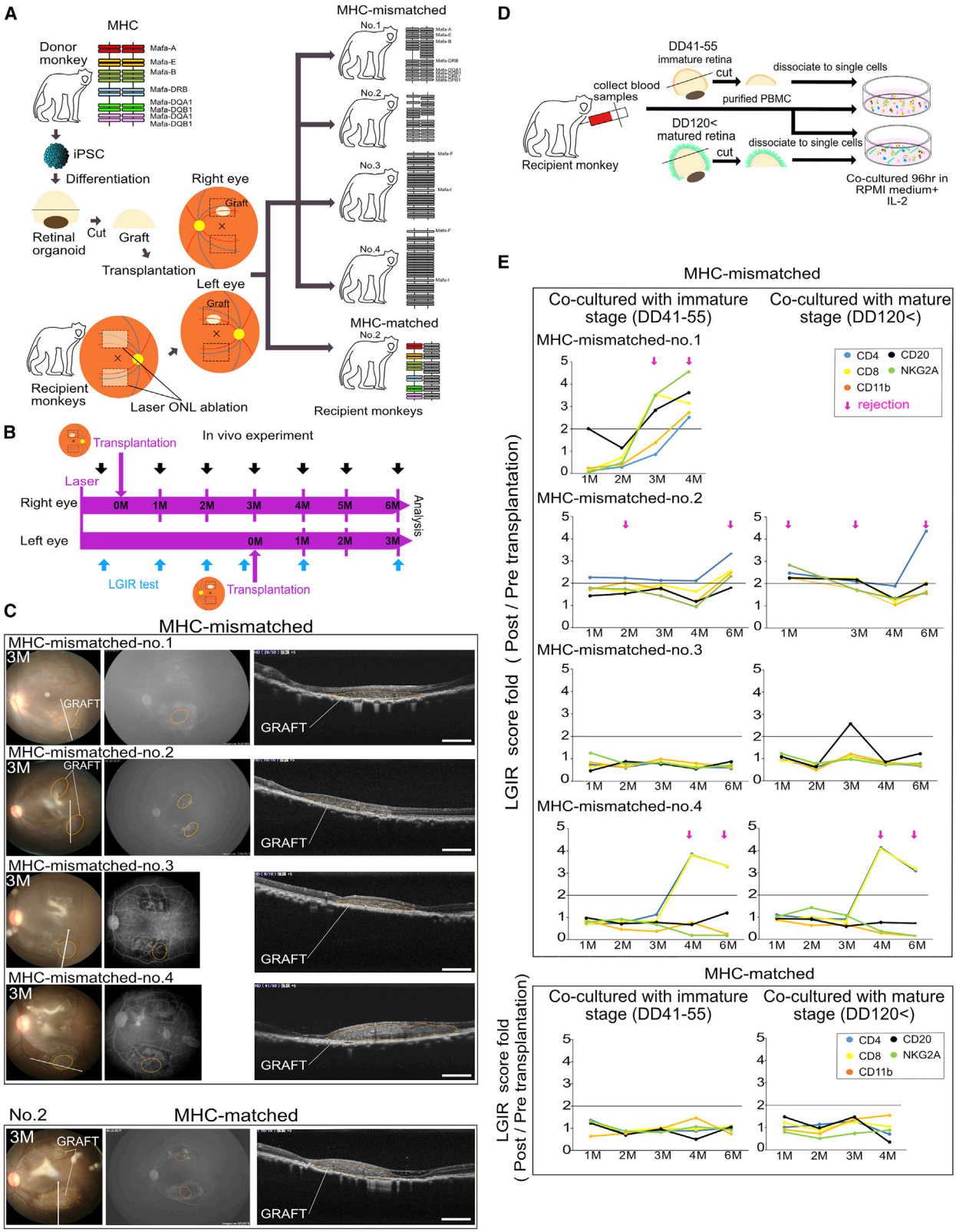

(legend on next page)

nos. 1 and 2 after the first transplantation and mismatched no.4 after the second transplantation; Figures 3D and 3E). As the grafts were transplanted at the retinal progenitor stage and further developed after transplantation, the LGIR test was conducted against the mkiPSC-retinas of both DD41–DD55 and DD120 <. The results were mostly consistent between the immature and developed retinas.

Transplanted grafts developed photoreceptors and expressed synapse markers irrespective of MHC matching

We then evaluated graft maturation using immunohistochemistry. A low-magnification image of the left eye (3 months after transplantation) of mismatched no.2 is representatively shown. Recoverin-positive photoreceptors were mostly deleted in the ONL-ablated area, and the graft was placed within the lesion (Figure 4A). Transplanted mkiPSC-retinas consistently developed recoverin/rhodopsin-positive photoreceptors in the left (3 months after transplantation) and right eyes (6 months after transplantation) of all MHC-matched and mismatched monkeys, except for the unexamined right eye of mismatched no.2, which developed retinal detachment after oil removal/cataract surgery at 5 months (Table 1). Well-organized photoreceptor rosettes expressed rhodopsin/cone opsins and peripherin II at the OS-like structures inside the rosette, whereas some disorganized rosettes expressed opsins on the cell membrane (Figures 4B and 4C″). The ratio of the well-organized rosettes varied from eye to eye, indicating that there may still be room for optimization in mkiPSC-retinal differentiation. Rarely, part of the mkiPSC-retinas developed a retina with a full IPL/INL/ONL, with the presence of photoreceptor synapses positive for CtBP2 and mGluR6 (mismatched no. 4; Figures 4D and 4E′). Pairs of pre-and postsynaptic markers CtBP2 and mGluR6 were also observed on the margin of the graft photoreceptor rosettes at the host-graft interface and inside the graft (MHC-matched no. 2; Figures 4F–4F‴).

Presence of activated MG was observed in MHC-matched and -mismatched transplantations

Next, we performed histological assessment of immune cell infiltration. Although subclinical immune rejection was indicated in three of four mismatched monkeys by LGIR, histologically, we observed no evident infiltration of CD3-positive T cells into the subretinal graft in these eyes. However, clusters of CD3-positive cells were observed in the displaced graft in the choroid, and the strayed graft was absent only in the MHC-mismatched monkey that was negative for LGIR (Figures 5A and 5B′; Table 1).

We then took a closer look at the MG by staining sections with a marker for Iba1. MG were present in both the MHC-mismatched and -matched grafts. Interestingly, most MG in the subretinal graft had ramified shapes (Figures 5C and 5D), while those in the displaced grafts in the choroid presented ameboid shapes (Figures 5A′ and 5B′). We then co-stained an activation marker, MHC class II, with Iba1 to determine whether there was site-specific MG activation in three regions: the transplant, untreated, and laser injury sites (Figures 5C′, 5C″, 5D′, and 5D″). MHC class II-positive MG were not observed in the untreated area, but some MG seemed activated in laser injury and transplant sites. We analyzed the degree of MG migration in the subretinal graft by quantifying the area of Iba1-positive regions within the grafts. There was no evident difference between the eyes due to the large variance (Figures 5E and 5F).

These results suggest that MG activation or accumulation was not evidently different between MHC-matched and -mismatched transplantation; however, activated MG after laser injury may trigger rejection in mismatched transplantation.

mESC-retina transplantation in an MHC-mismatched strain elicited host light responses to a lesser degree than matched transplantation

MHC class I molecules are expressed by neurons and contribute to synapse elimination or modification during

Figure 3. LGIR tests detected subclinical rejection in repeated MHC-mismatched transplantation

(A) Schematic overview of MHC homozygote mkiPSC-retina transplantation in 4 MHC-mismatched monkeys and 1 matched monkey.

(B) Experimental schedule of *in vivo* experiments and LGIR tests. The second transplantation (left eye) was planned 3 months after the first transplantation (right eye).

(C) *In vivo* images of the color fundus photographs and FAG and OCT images of the eyes that received the second transplantation 3 months after transplantation (see Figures S3 and S4 for the first eye images and for the different timings). Orange circles indicate graft areas. Each OCT image shows the sectional view of the line indicated by the white arrow on the color fundus image.

(D) Schematic image of LGIR test for the repeat experiment. Recipient PBMCs are co-cultured with mkiPSC-retinas at two developmental stages (DD41–DD55 and DD120<).

(E) Line plotting results for LGIR tests following transplantation. Vertical lines indicate post/pre-transplantation LGIR scores. Horizontal lines indicate months after transplantation. Magenta arrows show the time points when the post/pre-LGIR scores were above 2-fold in 2 or more cell types after transplantation (subclinical rejection).

LGIR test, lymphocyte graft immune reaction test; DD, differentiation day; FAG, fluorescein angiography; OCT, optical coherence tomography. Scale bars: (C) 1 mm.

Table 1. Summary of LGIR test and immunological features of transplanted eyes in histology

MHC	Mismatched								Matched		
Monkey number	1		2		3		4		1	2	
Operate eye	R	L	R	L	R	L	R	L	R	R	L
Postsurgical events	no		retinal detachment after cataract/oil removal surgery	no	cataract	no	no	retinal damage	no	no	no
Immunohistology	cryosection		cryosection	paraffin	cryosection	paraffin	cryosection	paraffin	cryosection	cryosection	paraffin
LGIR test	positive		positive		negative		positive		negative	negative	
Iba1-positive cell infiltration in choroidal tissue	+	+	ND	+	+	+	+	+	+	+	+
Iba1-positive cell infiltration in graft	+	+	ND	+	+	+	+	+	+	+	+
Graft maturation	+	+	ND	+	+	+	+	+	+	+	+
Strayed graft cells in choroid	+	–	ND	+	–	–	+	+	+	+	–
T cell infiltration in choroidal graft tissue	+	–	ND	+	–	–	+	+	–	–	–
T cell infiltration in subretinal graft	+/–	–	ND	–	–	–	–	–	–	–	–

ND, not determined. Indicated immunohistology was not evaluated in these eyes (mismatched 2R had retinal detachment). Immunohistology features the state of 6 months after transplantation in the right eye and 3 months after transplantation in the left eye.

CNS development (Huh et al., 2000), and MG are known to play a role in synapse maintenance (Wang et al., 2016). Thus, although MHC matching may not affect graft development, it may still affect functional host-graft integration. To investigate this, we used the mESC-retina of the C57BL/6J line that expresses CtBP2:tdTomato under the Nrl promoter (Matsuyama et al., 2021) and transplanted them into 10- to 12-week-old rd1-2J (C57BL/6J) and C3H/Hej mice with end-stage retinal degeneration (Figure 6A). The transplanted mice were administered indomethacin per our routine protocol; however, no immunosuppressive drugs were administered. The transplanted grafts developed recoverin- and rhodopsin-positive photoreceptor rosettes in both strains (Figure 6B). Host bipolar cells extended dendrites to graft rod photoreceptor cells expressing the reporter CtBP2:tdTomato in synaptic terminals (Figures 6B and 6B′), some of which were also stained for the postsynaptic marker mGluR6 (Figures 6C–6C″). CD3-positive lymphocyte infiltration was not evident at 14 or 28 days after transplantation in either strain, while Iba1-positive MG were present similarly around and inside photoreceptor rosettes in both strains (Figure S5). Retinas were then isolated for MEA recordings 8–10 weeks after transplantation. Figure 6D shows an example of a peristimulus time histogram of the host RGC light responses overlaid on the mapped graft location. The probabilities of host RGC responses to different light intensities from all retinas in each group are plotted in Figure 6E. We then modeled the response probability using a logistic regression as described previously (Matsuyama et al., 2021), considering the host (whether the transplanted animal was rd1-2j [matched] or C3H [mismatched]), stimulus strength (weak, medium, strong), L-AP4 treatment (before, L-AP4, after), sample bias, and spontaneous RGC firing (spiking rate before light stimulation). The transplanted retinas showed a higher probability of RGC responses to light than the untransplanted controls in both the rd1 and C3H samples, although the response probability was generally lower in C3H, i.e., mismatched, retinas (Figure S6).

DISCUSSION

Among cell-based therapies for degenerative diseases with a genetic background, allogeneic transplantation is the primary approach in which immunological control is an essential issue. We have previously shown that mESC/iPSC- and hESC-retinas can form synapses with host bipolar cells and significantly enhance light responses in host

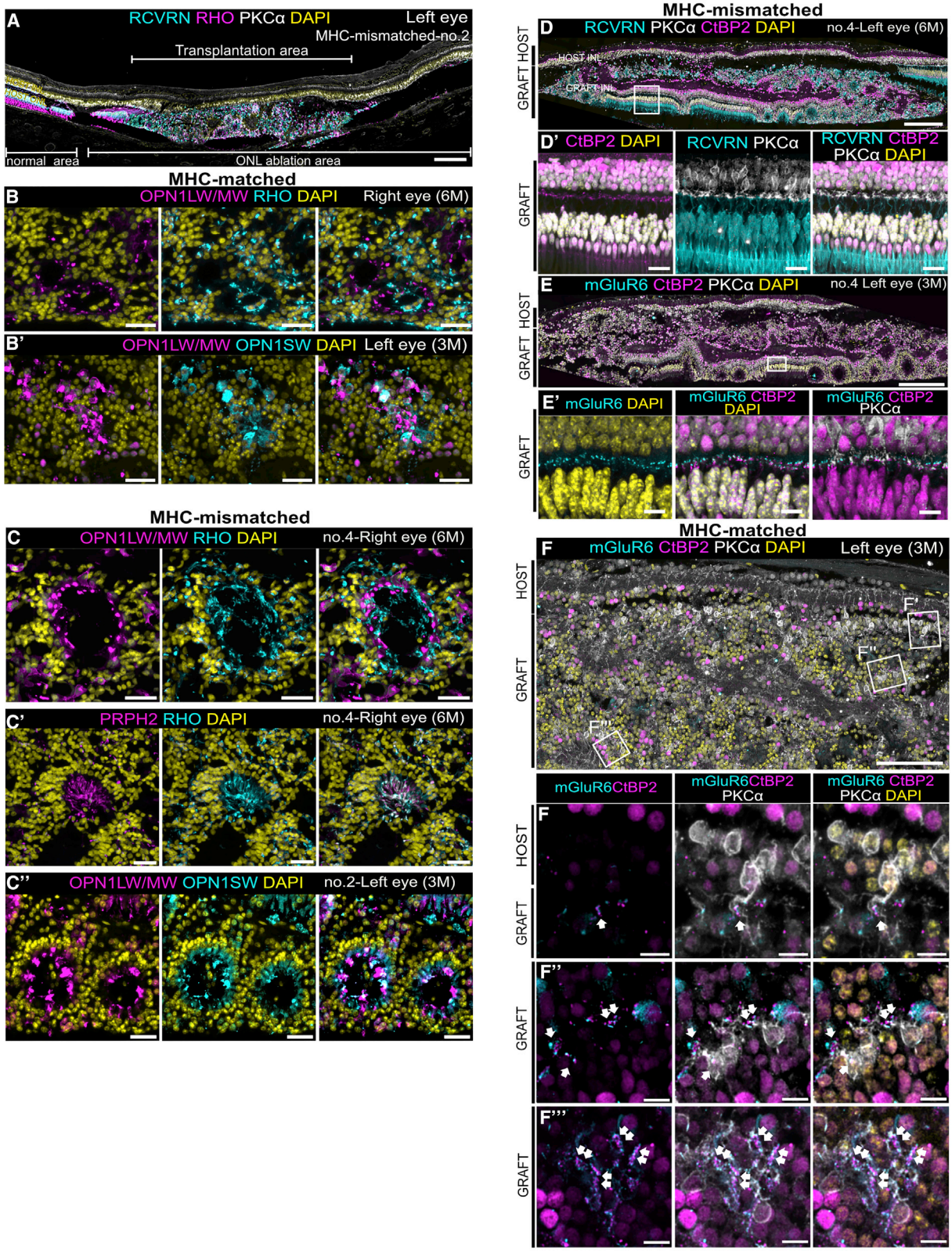

(legend on next page)

RGCs (Matsuyama et al., 2021; Yamasaki et al., 2022). In this study, we specifically investigated immunological responses in primates by optimizing a differentiation protocol for mkiPSC-retinas using homologous MHC cell lines to transplant them in MHC-matched or -mismatched monkeys. mkiPSC-retinas were functionally similar to hESC/iPSC-retinas in xeno-transplantation in rat retinal degeneration models, eliciting light responses in the host RGCs in roughly half of the transplanted rat retinas. The reason for this limited ratio is considered partly due to the presence of graft bipolar cells because genetic deletion of graft ON-bipolar cells in hESC-retinas further improved RGC responsiveness when transplanted in rats (Yamasaki et al., 2022).

Although the eye is an immune-privileged site, it is well estimated that in diseased eyes, the immunological environment is also altered when the blood-retinal barrier is impaired. Here, laser-induced ONL ablation disrupted the blood-retinal barrier (Berkowitz et al., 1991); however, transplants consistently developed rod- and cone-opsin-positive photoreceptor cells in both MHC-matched and -mismatched transplantations, even without immune suppression. However, using the LGIR test, three of four mismatched monkeys were judged to have subclinical rejection. LGIR has already been used in our clinical study of hiPSC-RPE transplantation for neovascular age-related macular degeneration (AMD), which sensitively detected immune rejection associated with a very early clinical manifestation (Sugita et al., 2020). Histologically, CD3 lymphocytes were rarely observed in the subretinal graft but were detected in or around the strayed grafts only in the choroid in mismatched monkey eyes. As we sometimes experienced technical difficulties inserting multiple grafts in these experiments, the strayed grafts could have been a surgical artifact, in addition to the effect of laser injury. Notably, strayed graft in choroid was absent only in the MHC-mismatched monkey that was negative for LGIR. This suggests that displaced allogenic grafts evoked immune responses outside the immune-privileged ocular site and that the LGIR test sensitively reflected these mild immune responses (Table 1). Inversely, disruption of the blood-retinal barrier by laser injury or mechanical surgical trauma could alter the immune-privileged environment and may increase the risk of subretinal graft rejection. From our limited results, we could not conclude that a second transplantation may boost the immune response. Altogether, despite the low immunogenicity and suppressive nature of hESC/iPSC-retinas, they may evoke an immune response, and LGIR may be a sensitive tool that detects such subclinical rejection. The use of immunosuppressants based on LGIR results may help prolong the survival of the graft. Additionally, LGIR tests using immature and developed retinas suggested that the risk of rejection did not seem to change according to the developmental stage of the graft after transplantation. It is also notable that in our LGIR tests, lymphocyte proliferation was initially suppressed shortly after transplantation in three of four mismatched monkeys. This may be consistent with our previous report that hESCs/iPSCs and monkey retinas actively suppress lymphocyte activation *in vitro* (Yamasaki et al., 2021).

Histologically, MG were consistently present in the grafts of both matched and mismatched transplantations. Retinal MG are important for immune modulation, such as antigen presentation, phagocytosis of dead cells, and pruning synapses in neural networks (Rathnasamy et al., 2019). MG in the graft may also eliminate damaged or non-integrating cells in the graft and contribute to host-graft or intra-graft synapse remodeling; however, they may also evoke host immune responses to donor-specific antigens. Here, MG were activated at the laser injury site in both MHC-mismatched and -matched eyes, implying that the blood-retinal barrier was disrupted by laser treatment. This may make MG more responsive to antigens in mismatched transplantations, and modulation of MG may reduce the risk of rejection.

A fully developed retina is rarely observed, typically appearing when the graft is young enough to develop a thick IPL/INL, such as in a DD30 graft that develops thick

Figure 4. Maturation of photoreceptors and photoreceptor synapses in the grafts for MHC-mismatched transplantation

(A) The low magnification image of the left eye of MHC-mismatched no. 2 representatively shows the ONL-ablated area and the graft.

(B and C) Graft photoreceptor rosettes in MHC-matched (B and B′) and mismatched (C–4C′′) eyes. OPN1SW/LW/MW and PRPH2 are localized at the outer segment-like structures inside the well-organized photoreceptor rosettes and are expressed on the cell membrane in disorganized rosettes.

(D and D′) Rarely, the graft develops an almost full retina with IPL and INL, including synapse formation within the graft, as suggested by the localization of the presynaptic marker CtBP2 at the contact site between graft bipolar dendrites and graft photoreceptor axons (mismatched no. 4). CtBP2 has a nuclear background staining. Magnified view of the box in (D) (D′).

(E and E′) The pre- and postsynaptic markers CtBP2 and mGluR6 were localized at the photoreceptor synapses in the same eye in (D). Magnified view of the box in (E) (E′).

(F–F′′′) Pairs of mGluR6 and CtBP2 (arrows) on the margin of the graft photoreceptor rosettes, adjacent to the host INL (F′) and within the graft (F′′). Magnified views of boxes in (F) (F′–F′′′).

Scale bars: (A, D, E, and F) 200 μm; (B, B′, and C– C′′) 30 μm; (D′, E′, and F′–F′′′) 20 μm.

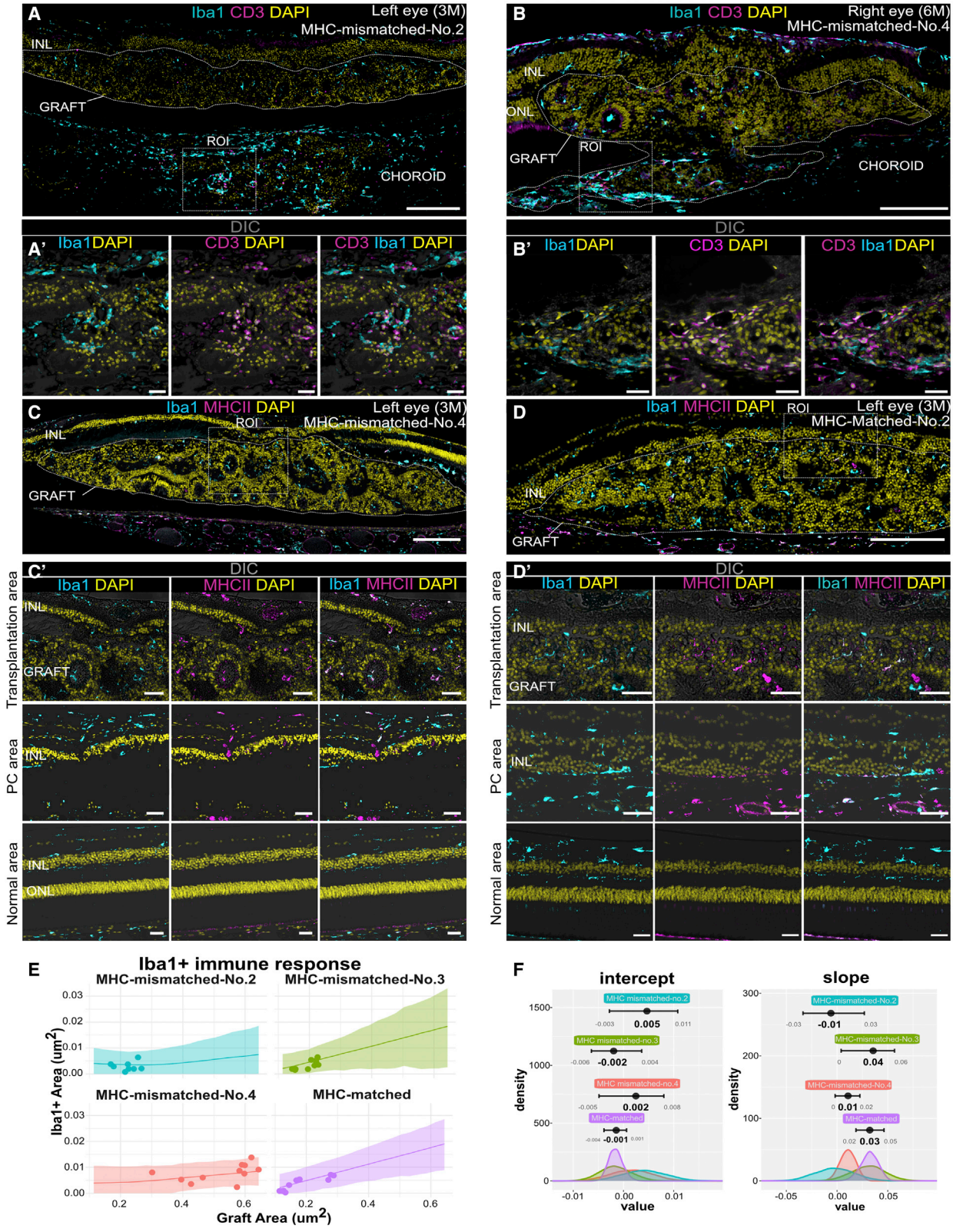

(legend on next page)

IPLs/INLs and large photoreceptor rosettes. These thick INL/IPL structures seem to block host-graft synaptic contact; therefore, we used a later-stage graft that could still form a photoreceptor layer, albeit mostly in a rosette form (Assawachananont et al., 2014; Shirai et al., 2016). These rosettes are considered disadvantageous in terms of retinoid cycling as they do not contact RPEs. However, host RGCs are ready to respond to light in MEA experiments without 9-*cis* retinal supplementation (Yamasaki et al., 2022), which implies that visual pigments are restored in photoreceptor cells, even in rosettes, after dark adaptation. This also suggests that the photoreceptor cells in rosettes can function *in vivo*. Additionally, Müller cells, which aid in retinoid recycling in cone photoreceptors, and horizontal cells, which are part of the photoreceptor triad synapses, are present in ESC/iPSC retina grafts (Matsuyama et al., 2021; Yamasaki et al., 2022). This implies that ESC/iPSC-retina provides a supportive environment for graft photoreceptor function. Interestingly, in our previous study, the expression of glial fibrillary acidic protein (GFAP) and/or HLA class I was enhanced in the non-integrating, reversely oriented parts of the rosettes. In addition, long-surviving graft photoreceptors presented hemispherical structures with the OSs correctly oriented toward the RPE, implying that the reversed parts of photoreceptor rosettes are prone to degeneration over time (Tu et al., 2019; Yamasaki et al., 2022).

Whether host and graft cells can form *de novo* synapses is a major concern in retinal sheet transplantation. We have shown the presence of host-graft synapse formation in mice with reporter bipolar cells and in a graft with the CtBP2-tdTomato reporter at the photoreceptor synaptic terminal (Mandai et al., 2017; Matsuyama et al., 2021). In another study, we used hESC-retinas with genetically reduced ON-bipolar cells, in which ON-bipolar cells of mostly host origin contacted graft photoreceptors presenting various pre-and postsynaptic markers (Yamasaki et al., 2022). These results suggest the potency of mkESC/iPSC-retinas to form host-graft synapses in monkey eyes, and our results showed that mkiPSC-retinas express photoreceptor synapse markers. However, it was difficult to clearly define the host-graft synapses in the present experimental setting.

Although MHC-mismatched transplantation seems acceptable, MHC molecules in the CNS are known to participate in synaptic pruning and the plasticity of the developing visual cortex in an activity-dependent manner (Zhang et al., 2013). Thus, we studied the functional aspects of MHC-matched and -mismatched mouse models. The overall mouse transplantation results were consistent with those of the monkey transplantations: there was no lymphocyte infiltration even with MHC-mismatched transplantation, and synaptic markers were present in the grafts of both MHC-matched and -mismatched transplantations, suggestive of host-graft synaptic contact. However, RGC light responsiveness was better in the C57BL/6 (matched) strain than in the C3H (mismatched) strain, possibly due to the MHC-matching process or differences in the pathological backgrounds of the host mice or in the host strain itself. If available, experiments using wild-type C3H grafts in rd1-2J and rd1(C3H) host mice would help clarify the effect of MHC matching on graft functional integration. We previously showed that C57BL/6J iPSC-retinas elicit host RGC light responses in immune-deficient NOG-rd1 mice, suggesting that host-graft functional integration is also achieved with MHC-mismatched transplantation, provided that immune rejection is controlled. Whether MHC matching affects the efficiency of functional integration requires further study.

In conclusion, we showed that in non-human primate (NHP) and mouse models, MHC-mismatched transplantation of ESC/iPSC-retinas could achieve graft maturation without evident clinical signs of rejection, even without systemic immune suppression, and that functional integration may be achieved. However, subclinical immune

Figure 5. Histological immune responses after transplantation

(A and B) Immunostaining of lymphocytes (CD3) and MG/macrophages (Iba1) at 3 months (MHC-mismatched no. 2, left eye) and 6 months (MHC-mismatched no. 4, right eye) after transplantation. Lymphocytes were barely observed in the subretinal graft, but lymphocytes and MG/macrophages were accumulated in the choroid near the graft (A, A′, B, and B′) or within the strayed graft in the choroid. Magnified view of the box in (A) and (B) (A′ and B′).

(C and D) Some MG co-localized with an activated marker MHC II in MHC-mismatched no. 4 and MHC-matched no. 2. Immunostaining of MG/MHC II in the graft, laser, and untreated areas, from top to bottom, with magnified view of graft site from the white box in (C) and (D) (C′ and D′). MG in the normal area is not activated, while some MGs were positive for MHC II at grafted and laser sites.

(E) Quantitative analysis of the glial area of Iba1-positive regions plotted against the areas of the grafts (dots). The model's (linear regression) posterior predictions are superimposed, with lines indicating the mean values and shaded areas indicating the 95% compatibility intervals.

(F) Posterior distributions for the intercept and slope of the linear regression, with bars on top indicating the mode and 95% compatibility intervals.

Scale bars: (A–D) 200 μm; (A′ and B′) 30 μm; (C′ and D′) 50 μm.

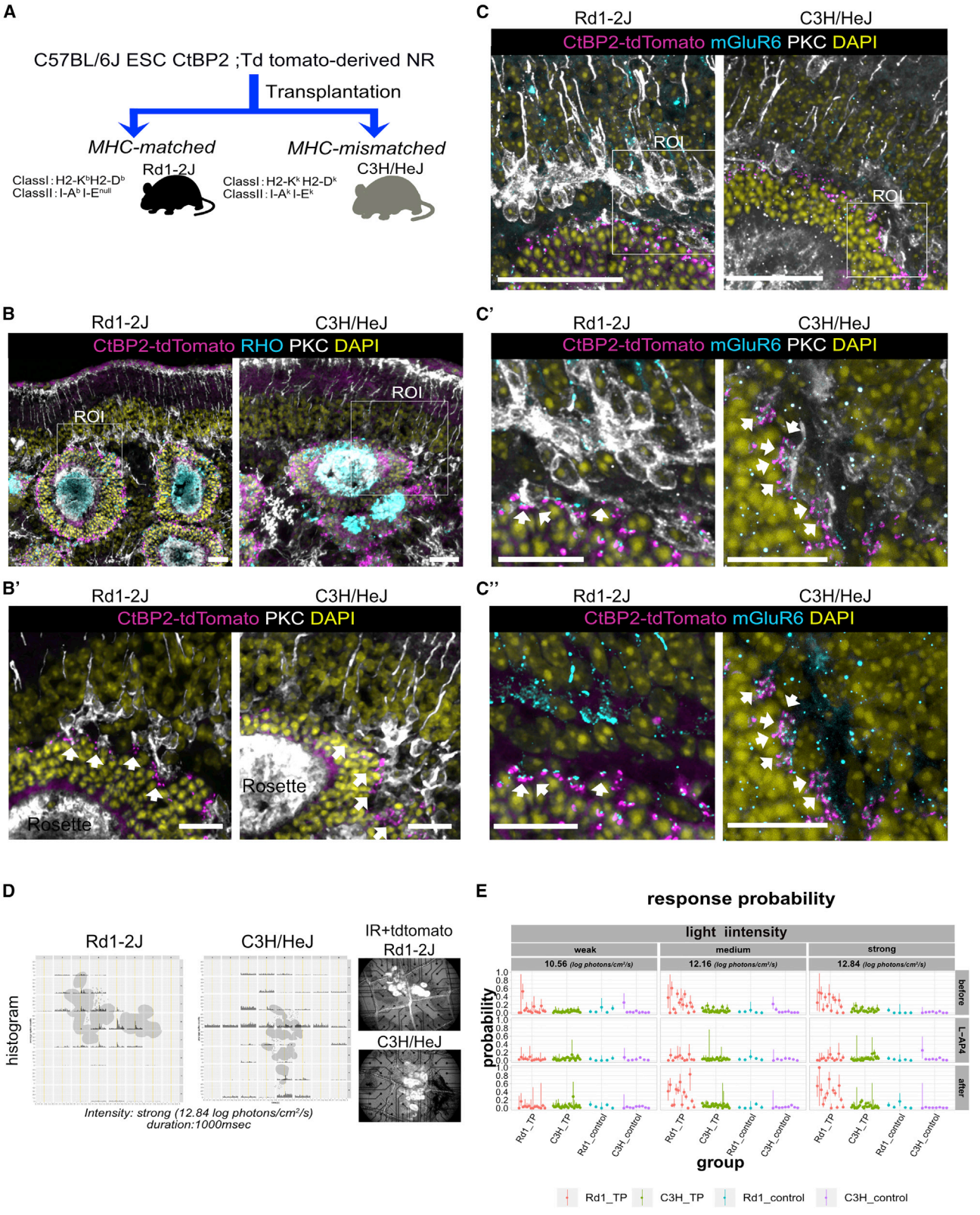

(legend on next page)

rejection has been implied by LGIR assays in MHC-mismatched transplantation in primates, which may affect long-term survival and functional integration. This suggests that with allogenic ESC/iPSC-retinal transplantation, even with stable graft survival, careful observation through LGIR monitoring is useful, and the effect of MHC matching on functional integration should be further investigated.

EXPERIMENTAL PROCEDURES

Animal experiments were approved by the RIKEN Biosystems Dynamics Research Ethics Committee (A2008-02-19). All animals were treated in accordance with the Association for Research in Vision and Ophthalmology Statement for Animals in Ophthalmology and Vision Research.

Animals

Cynomolgus macaques (*Macaca fascicularis*) were obtained from Ina-Research or Eve Bioscience. SD-Foxn1 Tg (S334ter) 3LavRrrc nude rats were obtained from the Rat Resource and Research Center. C3H/HeJ mice were obtained from Japan SLC, and rd1-2J mice were obtained from Jackson Laboratory. Animals were exposed to a 12 h light/dark cycle, and mice and rats had free access to food and water.

MHC typing of monkeys

Genotyping of two MHC-controlled monkeys (10154C, 9471 B) and two other monkeys (DrpZ11-34C-F, DpC16-8B-J) was conducted by Ina-Research, and the other monkeys were genotyped by Tokai University based on a previous report (Shiina et al., 2015).

Retinal organoid induction from mkiPSCs

The 1121A1 mkiPSC (HT1 homo) line was established and provided by the Center for iPS Cell Research and Application (CiRA) (Okamoto and Takahashi, 2011; Sugita et al., 2016). For retinal differentiation, based on previous reports, we adapted the serum-free floating culture of embryoid body-like aggregates through quick reaggregation (SFEBq) using induction-reversal culturing (Kuwahara et al., 2015; Nakano et al., 2012), with modifications. The detailed culture protocol is described in the supplemental experimental procedures.

LGIR test for monkeys

The detailed procedure of the LGIR test has been described previously and in the supplemental experimental procedures (Sugita et al., 2016). The LGIR test was conducted at the time points described for each experiment. PBMCs were isolated from the blood and stored at −80°C in CELLBANKER1 plus (Nippon Zenyaku Kogyo) freezing medium until use. Two different developmental stages of iPSC-retinas were used as immunogens: cells at DD41–DD55 as the retinal progenitor stage for transplantation, and cells at >DD120 as the more developed stage. We evaluated the ratio of Ki67-positive lymphocytes to other immune cell markers such as CD4-positive helper T cells, CD8-positive cytotoxic T cells, CD20-positive B cells, CD11b-positive monocytes/macrophages, and NKG2A-positive NK cells using flow cytometry. We evaluated the proliferating populations of these five types of immune cells among PBMCs co-cultured with mkiPSC-retinas. Compared with 0 W, it was considered as "rejection" when there was a 2-fold or greater Ki-67-positive population in at least two of the above cell types.

MEA recordings

As described previously and in the supplemental experimental procedures, MEA recordings were conducted with isolated retinas 8–10 weeks after transplantation using the USB-MEA60-Up-System (Multi-Channel Systems, Reutlingen, Germany) (Iraha et al., 2018; Tu and Matsuyama, 2020; Tu et al., 2019).

The procedures for the focal photoreceptor ablation in the monkey eyes, transplantation of mkiPSC-retinas in the monkey eyes, *in vivo* imaging after transplantation, quantification of Iba1-positive cells, statistical analysis, retinal organoid induction from mESCs, transplantation in rd1 mice, immunostaining, and analysis of MEA data are described in the supplemental experimental procedures.

SUPPLEMENTAL INFORMATION

Supplemental information can be found online at https://doi.org/10.1016/j.stemcr.2022.09.014.

Figure 6. C57BL/6J mouse ESC-derived retinas functionally integrate in the host rd1 C57BL/6J and C3H/HeJ mice

(A) Schematic images of experimental design for transplantation of mouse ESC-derived retinal organoids in rd1-2J (C57BL/6), i.e., matched or mismatched, mice.

(B and B′) Immunohistology of graft cells 4 weeks after transplantation. ESC-retinas have matured in both the rd1-2J and C3H/HeJ strains, and the dendrite tips of the host PKCα-positive bipolar cells contact the CtBP2:tdTomato reporter expressed at the synaptic terminal of the graft photoreceptors. Magnified views of the white box in (B) (B′).

(C–C″) Pairs of graft CtBP2:tdTomato reporter and mGluR6 immunostaining at the host rod bipolar dendrites. Magnification of white box in (C) (C′–C″).

(D) Representative peristimulus histograms at each channel, with overlaid graft mapping of the electrodes in the retinas of both host strains, of before, during, and after washing of pharmacological ON-blocker treatment.

(E) The probability that the RGCs would respond to light was plotted for each retina with three different light stimuli before, during, and after washing with L-AP4 treatment. This was performed in each group of two strains with and without transplantation (rd1-transplantation: n = 15; rd1-control: n = 5; C3H/HeJ-transplantation: n = 29; C3H/HeJ-control: n = 9).

Scale bars: (B and C) 50 μm; (B′, C′, and C″) 20 μm.

AUTHOR CONTRIBUTIONS

M.M., S.S., and M.T. designed and supervised this study. S.Y. and H.U. differentiated the mkiPSC-retinas. S.S. and H.U. conducted the LGIR tests. Y.K., H.U., T.W., and M.M. conducted the transplantation experiments. H.Y.T., H.U., and T.M. conducted the MEA experiments and analyses. H.U. and T.M. conducted the immunohistochemistry procedures and associated analyses. H.U., M.M., H.Y.T., T.M., and S.S. wrote the manuscript.

ACKNOWLEDGMENTS

This study was supported by a grant from the Japan Agency for Medical Research and Development (AMED) (grant number JP18bm0204002). The funds for the MHC-mismatched monkeys were provided by Sumitomo Pharma Co., Ltd. We thank M. Kawahara, J. Sho, T. Senba, T. Hashiguchi, K. Iseki, N. Hayashi, and S. Fujino for their support in experiments. We thank J. Takahashi and the CiRA for providing the 1121A1 iPSC line.

CONFLICTS OF INTERESTS

S.Y. is an employee at Sumitomo Pharma Co., Ltd. M.T. is a founder and the president of Vision Care, Inc., and a board member of Sysmex.

Received: December 24, 2021
Revised: September 28, 2022
Accepted: September 28, 2022
Published: October 27, 2022

REFERENCES

Assawachananont, J., Mandai, M., Okamoto, S., Yamada, C., Eiraku, M., Yonemura, S., Sasai, Y., and Takahashi, M. (2014). Transplantation of embryonic and induced pluripotent stem cell-derived 3D retinal sheets into retinal degenerative mice. Stem Cell Rep. *2*, 662–674. https://doi.org/10.1016/j.stemcr.2014.03.011.

Barber, A.C., Hippert, C., Duran, Y., West, E.L., Bainbridge, J.W., Warre-Cornish, K., Luhmann, U.F., Lakowski, J., Sowden, J.C., Ali, R.R., and Pearson, R.A. (2013). Repair of the degenerate retina by photoreceptor transplantation. Proc. Natl. Acad. Sci. USA *110*, 354–359. https://doi.org/10.1073/pnas.1212677110.

Barnea-Cramer, A.O., Wang, W., Lu, S.J., Singh, M.S., Luo, C., Huo, H., McClements, M.E., Barnard, A.R., MacLaren, R.E., and Lanza, R. (2016). Function of human pluripotent stem cell-derived photoreceptor progenitors in blind mice. Sci. Rep. *6*, 29784. https://doi.org/10.1038/srep29784.

Berkowitz, B.A., Sato, Y., Wilson, C.A., and de Juan, E. (1991). Blood-retinal barrier breakdown investigated by real-time magnetic resonance imaging after gadolinium-diethylenetriaminepentaacetic acid injection. Invest. Ophthalmol. Vis. Sci. *32*, 2854–2860.

Das, T., del Cerro, M., Jalali, S., Rao, V.S., Gullapalli, V.K., Little, C., Loreto, D.A., Sharma, S., Sreedharan, A., del Cerro, C., and Rao, G.N. (1999). The transplantation of human fetal neuroretinal cells in advanced retinitis pigmentosa patients: results of a long-term safety study. Exp. Neurol. *157*, 58–68. https://doi.org/10.1006/exnr.1998.6992.

Eiraku, M., Takata, N., Ishibashi, H., Kawada, M., Sakakura, E., Okuda, S., Sekiguchi, K., Adachi, T., and Sasai, Y. (2011). Self-organizing optic-cup morphogenesis in three-dimensional culture. Nature *472*, 51–56. https://doi.org/10.1038/nature09941.

Gasparini, S.J., Tessmer, K., Reh, M., Wieneke, S., Carido, M., Völkner, M., Borsch, O., Swiersy, A., Zuzic, M., Goureau, O., et al. (2022). Transplanted human cones incorporate into the retina and function in a murine cone degeneration model. J. Clin. Invest. *132*. https://doi.org/10.1172/jci154619.

Gonzalez-Cordero, A., West, E.L., Pearson, R.A., Duran, Y., Carvalho, L.S., Chu, C.J., Naeem, A., Blackford, S.J.I., Georgiadis, A., Lakowski, J., et al. (2013). Photoreceptor precursors derived from three-dimensional embryonic stem cell cultures integrate and mature within adult degenerate retina. Nat. Biotechnol. *31*, 741–747. https://doi.org/10.1038/nbt.2643.

Hori, J., Ng, T.F., Shatos, M., Klassen, H., Streilein, J.W., and Young, M.J. (2003). Neural progenitor cells lack immunogenicity and resist destruction as allografts. Stem Cell. *21*, 405–416. https://doi.org/10.1634/stemcells.21-4-405.

Huh, G.S., Boulanger, L.M., Du, H., Riquelme, P.A., Brotz, T.M., and Shatz, C.J. (2000). Functional requirement for class I MHC in CNS development and plasticity. Science *290*, 2155–2159. https://doi.org/10.1126/science.290.5499.2155.

Iraha, S., Tu, H.Y., Yamasaki, S., Kagawa, T., Goto, M., Takahashi, R., Watanabe, T., Sugita, S., Yonemura, S., Sunagawa, G.A., et al. (2018). Establishment of immunodeficient retinal degeneration model mice and functional maturation of human ESC-derived retinal sheets after transplantation. Stem Cell Rep. *10*, 1059–1074. https://doi.org/10.1016/j.stemcr.2018.01.032.

Keino, H., Horie, S., and Sugita, S. (2018). Immune privilege and eye-derived T-regulatory cells. J. Immunol. Res. *2018*, 1679197. https://doi.org/10.1155/2018/1679197.

Kuwahara, A., Ozone, C., Nakano, T., Saito, K., Eiraku, M., and Sasai, Y. (2015). Generation of a ciliary margin-like stem cell niche from self-organizing human retinal tissue. Nat. Commun. *6*, 6286. https://doi.org/10.1038/ncomms7286.

Kuwahara, A., Yamasaki, S., Mandai, M., Watari, K., Matsushita, K., Fujiwara, M., Hori, Y., Hiramine, Y., Nukaya, D., Iwata, M., et al. (2019). Preconditioning the initial state of feeder-free human pluripotent stem cells promotes self-formation of three-dimensional retinal tissue. Sci. Rep. *9*, 18936. https://doi.org/10.1038/s41598-019-55130-w.

MacLaren, R.E., Pearson, R.A., MacNeil, A., Douglas, R.H., Salt, T.E., Akimoto, M., Swaroop, A., Sowden, J.C., and Ali, R.R. (2006). Retinal repair by transplantation of photoreceptor precursors. Nature *444*, 203–207. https://doi.org/10.1038/nature05161.

Mandai, M., Fujii, M., Hashiguchi, T., Sunagawa, G.A., Ito, S.I., Sun, J., Kaneko, J., Sho, J., Yamada, C., and Takahashi, M. (2017). iPSC-derived retina transplants improve vision in rd1 end-stage retinal-degeneration mice. Stem Cell Rep. *8*, 69–83. https://doi.org/10.1016/j.stemcr.2016.12.008.

Matsuyama, T., Tu, H.-Y., Sun, J., Hashiguchi, T., Akiba, R., Sho, J., Fujii, M., Onishi, A., Takahashi, M., and Mandai, M. (2021).

Genetically engineered stem cell-derived retinal grafts for improved retinal reconstruction after transplantation. iScience *24*, 102866. https://doi.org/10.1016/j.isci.2021.102866.

Meyer, J.S., Howden, S.E., Wallace, K.A., Verhoeven, A.D., Wright, L.S., Capowski, E.E., Pinilla, I., Martin, J.M., Tian, S., Stewart, R., et al. (2011). Optic vesicle-like structures derived from human pluripotent stem cells facilitate a customized approach to retinal disease treatment. Stem Cell. *29*, 1206–1218. https://doi.org/10.1002/stem.674.

Morizane, A., Kikuchi, T., Hayashi, T., Mizuma, H., Takara, S., Doi, H., Mawatari, A., Glasser, M.F., Shiina, T., Ishigaki, H., et al. (2017). MHC matching improves engraftment of iPSC-derived neurons in non-human primates. Nat. Commun. *8*, 385. https://doi.org/10.1038/s41467-017-00926-5.

Nakano, T., Ando, S., Takata, N., Kawada, M., Muguruma, K., Sekiguchi, K., Saito, K., Yonemura, S., Eiraku, M., and Sasai, Y. (2012). Self-formation of optic cups and storable stratified neural retina from human ESCs. Cell Stem Cell *10*, 771–785. https://doi.org/10.1016/j.stem.2012.05.009.

Okamoto, S., and Takahashi, M. (2011). Induction of retinal pigment epithelial cells from monkey iPS cells. Invest. Ophthalmol. Vis. Sci. *52*, 8785–8790. https://doi.org/10.1167/iovs.11-8129.

Ortin-Martinez, A., Tsai, E.L., Nickerson, P.E., Bergeret, M., Lu, Y., Smiley, S., Comanita, L., and Wallace, V.A. (2017). A reinterpretation of cell transplantation: GFP transfer from donor to host photoreceptors. Stem Cell. *35*, 932–939. https://doi.org/10.1002/stem.2552.

Pearson, R.A., Barber, A.C., Rizzi, M., Hippert, C., Xue, T., West, E.L., Duran, Y., Smith, A.J., Chuang, J.Z., Azam, S.A., et al. (2012). Restoration of vision after transplantation of photoreceptors. Nature *485*, 99–103. https://doi.org/10.1038/nature10997.

Pearson, R.A., Gonzalez-Cordero, A., West, E.L., Ribeiro, J.R., Aghaizu, N., Goh, D., Sampson, R.D., Georgiadis, A., Waldron, P.V., Duran, Y., et al. (2016). Donor and host photoreceptors engage in material transfer following transplantation of post-mitotic photoreceptor precursors. Nat. Commun. *7*, 13029. https://doi.org/10.1038/ncomms13029.

Petersdorf, E.W. (2013). The major histocompatibility complex: a model for understanding graft-versus-host disease. Blood *122*, 1863–1872. https://doi.org/10.1182/blood-2013-05-355982.

Radtke, N.D., Seiler, M.J., Aramant, R.B., Petry, H.M., and Pidwell, D.J. (2002). Transplantation of intact sheets of fetal neural retina with its retinal pigment epithelium in retinitis pigmentosa patients. Am. J. Ophthalmol. *133*, 544–550. https://doi.org/10.1016/s0002-9394(02)01322-3.

Rathnasamy, G., Foulds, W.S., Ling, E.A., and Kaur, C. (2019). Retinal microglia - a key player in healthy and diseased retina. Prog. Neurobiol. *173*, 18–40. https://doi.org/10.1016/j.pneurobio.2018.05.006.

Reichman, S., Slembrouck, A., Gagliardi, G., Chaffiol, A., Terray, A., Nanteau, C., Potey, A., Belle, M., Rabesandratana, O., Duebel, J., et al. (2017). Generation of storable retinal organoids and retinal pigmented epithelium from adherent human iPS cells in xeno-free and feeder-free conditions. Stem Cell. *35*, 1176–1188. https://doi.org/10.1002/stem.2586.

Ribeiro, J., Procyk, C.A., West, E.L., O'Hara-Wright, M., Martins, M.F., Khorasani, M.M., Hare, A., Basche, M., Fernando, M., Goh, D., et al. (2021). Restoration of visual function in advanced disease after transplantation of purified human pluripotent stem cell-derived cone photoreceptors. Cell Rep. *35*, 109022. https://doi.org/10.1016/j.celrep.2021.109022.

Santos-Ferreira, T., Llonch, S., Borsch, O., Postel, K., Haas, J., and Ader, M. (2016). Retinal transplantation of photoreceptors results in donor-host cytoplasmic exchange. Nat. Commun. *7*, 13028. https://doi.org/10.1038/ncomms13028.

Seiler, M.J., Aramant, R.B., Jones, M.K., Ferguson, D.L., Bryda, E.C., and Keirstead, H.S. (2014). A new immunodeficient pigmented retinal degenerate rat strain to study transplantation of human cells without immunosuppression. Graefes Arch. Clin. Exp. Ophthalmol. *252*, 1079–1092. https://doi.org/10.1007/s00417-014-2638-y.

Shiba, Y., Gomibuchi, T., Seto, T., Wada, Y., Ichimura, H., Tanaka, Y., Ogasawara, T., Okada, K., Shiba, N., Sakamoto, K., et al. (2016). Allogeneic transplantation of iPS cell-derived cardiomyocytes regenerates primate hearts. Nature *538*, 388–391. https://doi.org/10.1038/nature19815.

Shiina, T., Yamada, Y., Aarnink, A., Suzuki, S., Masuya, A., Ito, S., Ido, D., Yamanaka, H., Iwatani, C., Tsuchiya, H., et al. (2015). Discovery of novel MHC-class I alleles and haplotypes in Filipino cynomolgus macaques (Macaca fascicularis) by pyrosequencing and Sanger sequencing: Mafa-class I polymorphism. Immunogenetics *67*, 563–578. https://doi.org/10.1007/s00251-015-0867-9.

Shirai, H., Mandai, M., Matsushita, K., Kuwahara, A., Yonemura, S., Nakano, T., Assawachananont, J., Kimura, T., Saito, K., Terasaki, H., et al. (2016). Transplantation of human embryonic stem cell-derived retinal tissue in two primate models of retinal degeneration. Proc. Natl. Acad. Sci. USA *113*, E81–E90. https://doi.org/10.1073/pnas.1512590113.

Singh, M.S., Balmer, J., Barnard, A.R., Aslam, S.A., Moralli, D., Green, C.M., Barnea-Cramer, A., Duncan, I., and Maclaren, R.E. (2016). Transplanted photoreceptor precursors transfer proteins to host photoreceptors by a mechanism of cytoplasmic fusion. Nature *7*, 13537. https://doi.org/10.1038/ncomms13537.

Singh, M.S., Charbel Issa, P., Butler, R., Martin, C., Lipinski, D.M., Sekaran, S., Barnard, A.R., and MacLaren, R.E. (2013). Reversal of end-stage retinal degeneration and restoration of visual function by photoreceptor transplantation. Proc. Natl. Acad. Sci. USA *110*, 1101–1106. https://doi.org/10.1073/pnas.1119416110.

Streilein, J.W. (2003). Ocular immune privilege: therapeutic opportunities from an experiment of nature. Nat. Rev. Immunol. *3*, 879–889. https://doi.org/10.1038/nri1224.

Sugita, S., Iwasaki, Y., Makabe, K., Kamao, H., Mandai, M., Shiina, T., Ogasawara, K., Hirami, Y., Kurimoto, Y., and Takahashi, M. (2016). Successful transplantation of retinal pigment epithelial cells from MHC homozygote iPSCs in MHC-matched models. Stem Cell Rep. *7*, 635–648. https://doi.org/10.1016/j.stemcr.2016.08.010.

Sugita, S., Mandai, M., Hirami, Y., Takagi, S., Maeda, T., Fujihara, M., Matsuzaki, M., Yamamoto, M., Iseki, K., Hayashi, N., et al. (2020). HLA-matched allogeneic iPS cells-derived RPE transplantation for macular degeneration. J. Clin. Med. *9*. https://doi.org/10.3390/jcm9072217.

Tu, H.-Y., and Matsuyama, T. (2020). Multielectrode Array Recording of Mouse Retinas Transplanted with Stem Cell-Derived Retinal Sheets (Springer US), pp. 207–220. https://doi.org/10.1007/978-1-0716-0175-4_15.

Tu, H.Y., Watanabe, T., Shirai, H., Yamasaki, S., Kinoshita, M., Matsushita, K., Hashiguchi, T., Onoe, H., Matsuyama, T., Kuwahara, A., et al. (2019). Medium- to long-term survival and functional examination of human iPSC-derived retinas in rat and primate models of retinal degeneration. EBioMedicine *39*, 562–574. https://doi.org/10.1016/j.ebiom.2018.11.028.

Umekage, M., Sato, Y., and Takasu, N. (2019). Overview: an iPS cell stock at CiRA. Inflamm. Regen. *39*, 17. https://doi.org/10.1186/s41232-019-0106-0.

Waldron, P.V., Di Marco, F., Kruczek, K., Ribeiro, J., Graca, A.B., Hippert, C., Aghaizu, N.D., Kalargyrou, A.A., Barber, A.C., Grimaldi, G., et al. (2018). Transplanted donor- or stem cell-derived cone photoreceptors can both integrate and undergo material transfer in an environment-dependent manner. Stem Cell Rep. *10*, 406–421. https://doi.org/10.1016/j.stemcr.2017.12.008.

Wang, X., Zhao, L., Zhang, J., Fariss, R.N., Ma, W., Kretschmer, F., Wang, M., Qian, H.H., Badea, T.C., Diamond, J.S., et al. (2016). Requirement for microglia for the maintenance of synaptic function and integrity in the mature retina. J. Neurosci. *36*, 2827–2842. https://doi.org/10.1523/JNEUROSCI.3575-15.2016.

Warre-Cornish, K., Barber, A.C., Sowden, J.C., Ali, R.R., and Pearson, R.A. (2014). Migration, integration and maturation of photoreceptor precursors following transplantation in the mouse retina. Stem Cell. Dev. *23*, 941–954. https://doi.org/10.1089/scd.2013.0471.

Yamasaki, S., Sugita, S., Horiuchi, M., Masuda, T., Fujii, S., Makabe, K., Kawasaki, A., Hayashi, T., Kuwahara, A., Kishino, A., et al. (2021). Low immunogenicity and immunosuppressive properties of human ESC- and iPSC-derived retinas. Stem Cell Rep. *16*, 851–867. https://doi.org/10.1016/j.stemcr.2021.02.021.

Yamasaki, S., Tu, H.Y., Matsuyama, T., Horiuchi, M., Hashiguchi, T., Sho, J., Kuwahara, A., Kishino, A., Kimura, T., Takahashi, M., and Mandai, M. (2022). A Genetic modification that reduces ON-bipolar cells in hESC-derived retinas enhances functional integration after transplantation. iScience *25*, 103657. https://doi.org/10.1016/j.isci.2021.103657.

Zhang, A., Yu, H., Shen, Y., Liu, J., He, Y., Shi, Q., Fu, B., Miao, F., and Zhang, J. (2013). The expression patterns of MHC class I molecules in the developmental human visual system. Neurochem. Res. *38*, 273–281. https://doi.org/10.1007/s11064-012-0916-9.

Zhong, X., Gutierrez, C., Xue, T., Hampton, C., Vergara, M.N., Cao, L.-H., Peters, A., Park, T.S., Zambidis, E.T., Meyer, J.S., et al. (2014). Generation of three-dimensional retinal tissue with functional photoreceptors from human iPSCs. Nat. Commun. *5*, 1–14. https://doi.org/10.1038/ncomms5047.